Numerical investigation of the cavitation effect on natural frequencies of a hydrofoil

Xin Liu[1], Lingjiu Zhou[2]*, Xavier Escaler[3], Zhengwei Wang[1]

ISROMAC 2016

International Symposium on Transport Phenomena and Dynamics of Rotating Machinery

Hawaii, Honolulu

April 10-15, 2016

Abstract

The added mass effects on a NACA0009 hydrofoil under cavitation conditions determined in a cavitation tunnel have been numerically simulated using finite element method (FEM). Based on the validated model, the effects of averaged properties of the cavity considered as a two-phase mixture have been evaluated. the simulation results point out that the average properties of the cavity, considered as a mixture of vapor/water, have a significant effect on added mass coefficients and mode shapes. These effects appear to be more important for higher modes of vibration. For instance, the first torsion mode can evolve towards the second bending mode when reducing the cavity void ratio from 1 to 0.9.

Keywords

Added mass — Sheet cavitation — Fluid-structure interaction — Mode transition

[1] *Department of Thermal Engineering, Tsinghua University, Beijing, China*

[2] *College of Water Resources & Civil Engineering, China Agricultural University, Beijing, China*

[3] *Center for Industrial Diagnostics, Universitat Politècnica de Catalunya, Barcelona, Spain*

***Corresponding author**: zlj@cau.edu.cn

INTRODUCTION

If large scale cavitation attaches to a solid surface, additional uncertainties will be added to the FSI (Fluid-Structure Interaction) phenomenon. Both cavitation flow and classic FSI problems have been studied for years separately, but it is still a challenge to estimate added mass effects in a cavitation flow. The mixture of water and vapor phases that forms the macroscopic hydrodynamic cavities can create averaged properties that are difficult to quantify and that vary from the expected effects of pure liquid water flow. Moreover, new boundary conditions at cavitation regions are not fully understood. In fact, many studies have noted the cavitation effects on FSI for various bodies, especially propeller blades and hydrofoils. Nevertheless, estimations of such effects are only seldom found.

The FEM-based acoustic fluid approach, that avoids the modeling effort and the time duration of the 2-way FSI simulation, can be easily applied to model complex structural and fluid geometries with high efficiency particularly at the design stage for safety assessment. In spite of that, this method has not yet been used to estimate the added mass effects on hydrofoils under cavitation conditions due to the difficulties of modelling the cavity properties.

The added mass effects under cavitation conditions on a NACA0009 hydrofoil determined in a cavitation tunnel will be numerically simulated using finite element method (FEM). A coupled acoustic fluid-structural system comprising the tunnel test section will be solved for different fluid conditions. The numerical results for a NACA0009 hydrofoil with partial cavitation have been compared with the experimental ones obtained by De La Torre, et al. [1]. The hydrofoil modes of vibration will be determined for only air, only water and for various vapor-water conditions. In particular, several leading edge attached partial cavities with different dimensions and made of pure vapor will be simulated.

1. METHODS

In FSI problems, the structural dynamics equation must be considered along with the Navier-Stokes (NS) and the continuity equations. The discretized structural dynamics equation can be formulated based on the structural elements. The NS and continuity equations are simplified to get the acoustic wave equation assuming that the fluid is compressible, which means that its density changes due to pressure variations (i.e. acoustic medium), and that there is no fluid flow [2].

The governing finite element matrix equations of multiphase FSI are expressed in Equation (1):

$$\begin{bmatrix} [M_S] & 0 & 0 \\ \bar{\rho}_{0,liquid}[R_{liquid}]^T & [M_{F,liquid}] & 0 \\ \bar{\rho}_{0,gas}[R_{gas}]^T & 0 & [M_{F,gas}] \end{bmatrix} \begin{Bmatrix} \{\ddot{u}\} \\ \{\ddot{p}_{liquid}\} \\ \{\ddot{p}_{gas}\} \end{Bmatrix} + \begin{bmatrix} [C_S] & 0 & 0 \\ 0 & [C_{F,liquid}] & 0 \\ 0 & 0 & [C_{F,gas}] \end{bmatrix} \begin{Bmatrix} \{\dot{u}\} \\ \{\dot{p}_{liquid}\} \\ \{\dot{p}_{gas}\} \end{Bmatrix} + \begin{bmatrix} [K_S] & -[R_{liquid}] & -[R_{gas}] \\ 0 & [K_{F,liquid}] & 0 \\ 0 & 0 & [K_{F,gas}] \end{bmatrix} \begin{Bmatrix} \{u\} \\ \{p_{liquid}\} \\ \{p_{gas}\} \end{Bmatrix} = \begin{Bmatrix} F_S \\ F_{F,liquid} \\ F_{F,gas} \end{Bmatrix} \quad (1)$$

where M_F, C_F and K_F are the fluid mass, damping and stiffness matrices, respectively. R is a coupling matrix that represents the effective surface area associated with each node on the fluid-structure interface. F_F is the applied fluid pressure vector at the interface obtained by integrating the pressure over the area of the surface. P and U are the fluid pressure and the structure displacement vectors, respectively. M_S, C_S and K_S are the structure mass, damping and stiffness matrices, respectively, and F_S is the structural load vector.

2. Numerical Model

The simulated case corresponds to a NACA0009 hydrofoil, as shown in Figure 1, under various cavitation conditions experimentally tested at the EPFL High-Speed Cavitation Tunnel. On the left of Figure 3, a photograph of the typical attached partial cavitation as described in De La Torre, et al. [1] is shown. The foil is made of aluminum alloy with a Young's modulus of 0.54 GPa, a Poisson's ratio of 0.33 and a density of 2770 kg/m^3.

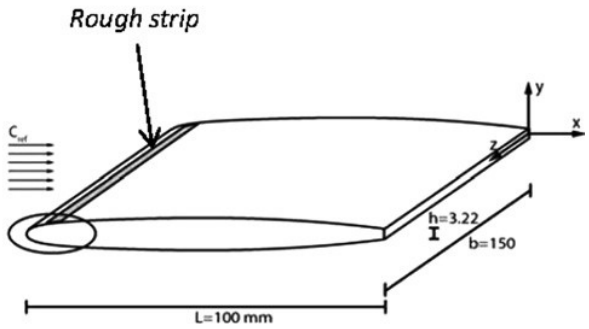

Figure 1. Truncated NACA0009 hydrofoil.

The FSI domain, which comprises the whole test section of the cavitation tunnel, was meshed with hexahedral elements as shown in Figure 2. The hydrofoil was fixed with an incidence angle of 0º.

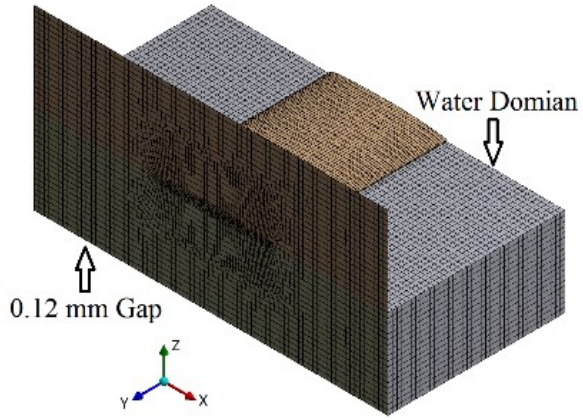

Figure 2. Discretized finite element mesh of the FSI domain with the surrounding water.

One lateral section of the hydrofoil was constrained in the model. The rest of hydrofoil surfaces were in contact with the fluid. A FSI condition was set at these interfaces so that the displacement of the structure is identical to that of the fluid in normal direction. Considering the coupling characteristics of vibration in water, the fluid boundaries were modeled as fully reflective. The water properties were set as 1000 kg/m^3 for density and 1450 m/s for speed of sound.

Regarding the modelling of the attached cavity, it was considered to be of a constant length along the whole span as shown on Figure 3. Acoustic elements were used like for the water domain. At the interface of the vapor cavity with the surrounding water, the acoustic pressure and the normal component of the water/vapor velocity are continuous. The vapor properties were set as 0.174 kg/m^3 for density and 340 m/s for speed of sound.

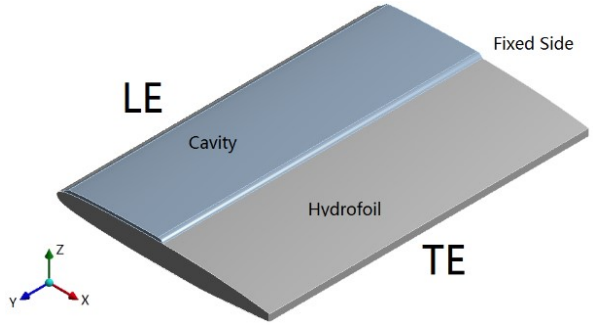

Figure 3. Lateral view of the cavity numerical model.

For simplification purposes, the simulated cavity represents a constant thickness and length domain which obviously differs from the actual cavity shape. Regarding the cavity thickness, that could not be measured during the experiments, the visual impression was that it was quite constant, as shown in Figure 4.

Figure 4. View of the cavitation from the top.

3. Results and Discussion

The effects on the added mass coefficients and on the mode shapes have been evaluated when the cavity is assumed to be a two-phase mixture. During the experiments in the cavitation tunnel, De La Torre et al. [1] observed that the attached cavity morphology was not homogeneous. In most

of the cases, two different regions, named as transparent and foamy, could be identified depending on the visual aspect. The transparent region was considered to be mainly composed by a single phase of vapor and the foamy one was considered to be mainly composed by a homogeneous mixture of vapor and water.

In our cavity model, it is possible to simulate a non-pure vapor cavity by assuming the averaged properties of a two-phase flow based on the void fraction, α, which is defined as:

$$\alpha = \frac{V_V}{V} \tag{2}$$

where V_V is the vapor volume and V is the total volume of the cavity. Consequently, the cavity density, ρ_c, can now be calculated as:

$$\rho_c = \alpha\rho_V + (1-\alpha)\rho_L \tag{3}$$

where ρ_V is a vapor density of and ρ_L is the water density, which have been taken as $1.74 \cdot 10^{-2}$ (saturated vapor at 20 °C) and as 1000 kg/m^3, respectively.

The speed of sound in a bubbly air/water mixture at atmospheric pressure tested by Brennen [3] as well as the cavity density are plotted in Figure 5 as a function of void fraction. These data have been taken as the reference values to carry out the numerical simulations with a cavity of fixed length (*l*/*c* = 0.318) detaching from the leading edge and fixed width of 1.8 mm.

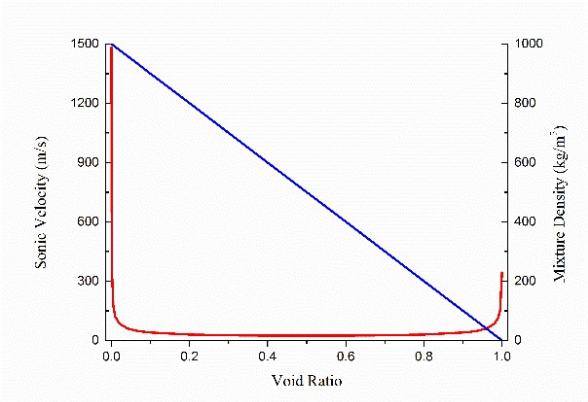

Figure 5. Speed of sound in a bubbly air/water mixture at atmospheric pressure and cavity density as a function of void ratio.

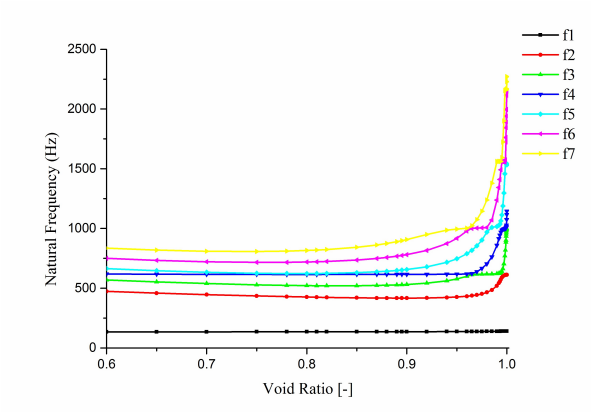

Figure 6. Natural frequency evolution as a function of cavity void ratio for first seven order modes.

The significant differences in the f3 mode shapes shown in Figure 7 between the air and cavitation conditions obtained with the acoustic model are in close agreement with experimental measurements.

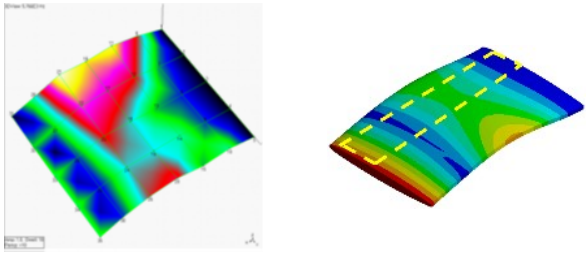

Figure 7. Measured and predicted f3 mode shapes.

Based on such data from Brennen, a series of cases have been simulated considering the void ratio in the range from 0.6 to 1 as shown on Figure 6. When the void ratio is below 0.9, the natural frequency of each mode does not change significantly. But when the void ratio is larger than 0.9, particularly above 0.99, the natural frequency of each mode changes sharply. The mode transition, as shown as in Figure 8 and Figure 9, exits but cannot distinguished easily. Moreover, the mode transition can happen more than once for the same order mode, such as f_5, f_6 and f_7.

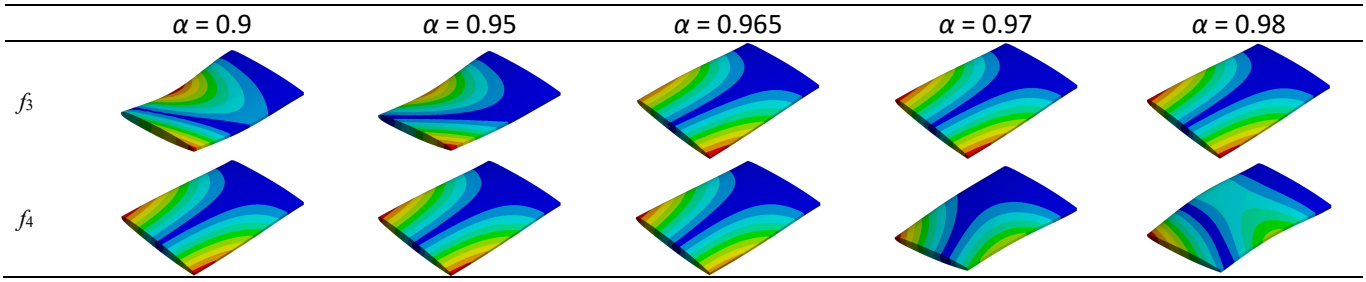

Figure 8. Example of the first kind of mode transitions for f_3 and f_4, and some modal shapes at particular void ratios.

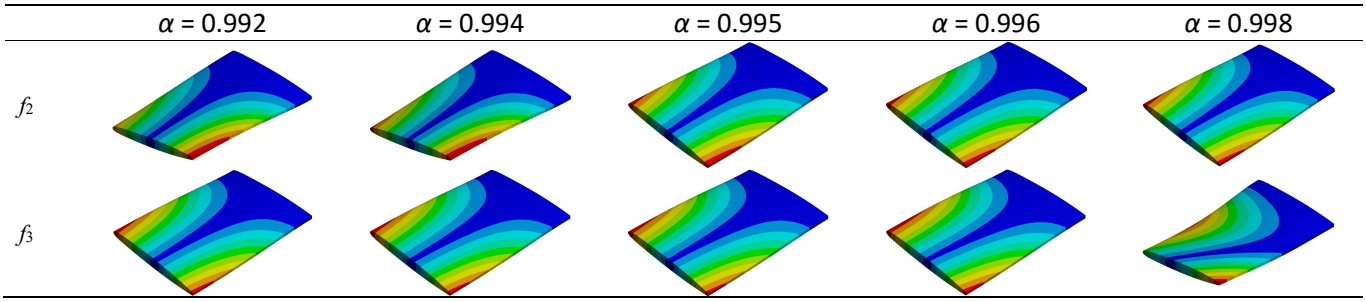

Figure 9. Example of the first kind of mode transitions for f_2 and f_3, and some modal shapes at particular void ratios.

The two modes of transition can intersect at a narrow frequency range. For example, as shown in Figure 7, the intersection void ratio is 0.965; before this value, the frequency and modal shape of f_4 keep unchanged while the frequency and modal shape of $f3$ is approaching to f_4 along with the void ratio increase. At α = 0.965, $f3$ and f_4 have a very close frequency and almost the same shapes. After 0.965, it turns that the $f3$ is unchanged while f_4 begins to change both frequency and modal shapes.

4. Conclusion

The added mass effects on a NACA0009 hydrofoil under cavitation conditions have been numerically calculated using acoustic FEM. The simulation results point out that the average properties of the cavity, considered as a mixture of vapor/water, have a significant effect on added mass coefficients and mode shapes. These effects appear to be more important for higher modes of vibration. For instance, the second bending mode can evolve towards a second bending mode when reducing the cavity void ratio from 1 to 0.9.

ACKNOWLEDGMENTS

This work was supported by National Natural Science Foundation of China (Nos. 51279083 and 51409148).

REFERENCES

[1] O. De La Torre, X. Escaler, E. Egusquiza and M. Farhat. Experimental investigation of added mass effects on a hydrofoil under cavitation conditions. Journal of Fluids and Structures, 39:173-187, 2013.

[2] ANSYS Inc. Ansys theory reference (Ansys), 2013.

[3] C. E. Brennen. Homogeneous bubbly flows - in Cavitation and bubble dynamics. Oxford: Oxford University Press, 1995.